

# Generic Contrast Agents

Our portfolio is growing to serve you better. Now you have a *choice*.



[VIEW CATALOG](#)

# AJNR

## **Differential effects of age and sex on the cerebellar hemispheres and the vermis: a prospective MR study.**

N Raz, J H Dupuis, S D Briggs, C McGavran and J D Acker

*AJNR Am J Neuroradiol* 1998, 19 (1) 65-71

<http://www.ajnr.org/content/19/1/65>

This information is current as of May 29, 2025.

## Differential Effects of Age and Sex on the Cerebellar Hemispheres and the Vermis: A Prospective MR Study

Naftali Raz, James H. Dupuis, Susan D. Briggs, Catherine McGavran, and James D. Acker

**PURPOSE:** The purpose of this study was to determine the effects of age and sex on the size of the cerebellar hemispheres, the cerebellar vermis, and the pons in healthy adults.

**METHODS:** We estimated the volumes of the cerebellar hemispheres (excluding the vermis and the peduncles), the cross-sectional area of the vermis, and the cross-sectional area of the ventral pons from MR images obtained in 146 healthy volunteers, 18 to 77 years old.

**RESULTS:** We found a mild but significant age-related reduction in the volume of the cerebellar hemispheres and in the total area of the cerebellar vermis; however, the analysis of age trends in the vermis lobules revealed differential age-related declines. The areas of lobules VI and VII and of the posterior vermis lobules (VIII–X) declined significantly with age, whereas the anterior vermis (I–V) showed no significant age-related shrinkage. The volume of the cerebellar hemispheres (especially the right) and the area of the anterior vermis were greater in men, even after adjustment for height. Neither age nor sex affected the area of the ventral pons.

**CONCLUSIONS:** Normal aging of the cerebellum is associated with selective regional shrinkage. The cerebellar hemispheres and the area of the anterior vermis may be larger in men than in women regardless of differences in body size.

Aging of the human brain is a differential process in which significant deterioration in some regions coexists with relative preservation in others (1–3). Although this pattern is apparent in the cerebral cortex, it is unclear whether it can be extended to the structures of the posterior fossa. Moderate shrinkage of the cerebellar hemispheres has been observed in postmortem examinations (4, 5) and in in vivo investigations (6–10). Differential aging of the cerebellar vermis involving lobules VI and VII and to some

extent lobules VIII through X, but not the anterior cerebellar vermis, has also been reported (7, 11). In one study, however, an opposite pattern was observed, that is, a significant negative age trend was found for the anterior but not the posterior vermis (12). In contrast to the cerebellum, the pons has consistently been shown to maintain its gross size throughout the life span (9, 11–14). Several investigators have observed sex differences in gross cerebellar neuroanatomy. Men were shown to have larger cerebella than those of age-matched women, although in these reports the possibility that these differences could have reflected sexual dimorphism of body size was not consistently ruled out. Men also evidenced significantly larger pons areas in at least one sample (11).

In the prospective study reported here, we examined age and sex differences in the size of the cerebellum and the ventral pons. Our main hypothesis was that in the healthy elderly, the cerebellar hemispheres and lobules VI and VII of the vermis would show age-related shrinkage whereas the anterior vermis and pons would not. In addition, we hypothesized that with body size controlled, there would be no sex differences in the size of the cerebellum and pons.

---

Received March 11, 1997; accepted after revision June 17.

Presented in part at the annual meeting of the European Neuroscience Association, Vienna, Austria, August 1994, and at the annual meeting of the Society for Neuroscience, San Diego, Calif, November 1995.

Supported in part by National Institutes of Health grant AG-11230 to Dr. Raz and by the Center of Excellence grant to the Department of Psychology of the University of Memphis from the state of Tennessee.

From the Department of Psychology, University of Memphis (Tenn) (N.R., J.H.D., S.D.B., C.M.G.), and Baptist MR Diagnostic Imaging Center, Baptist Memorial Hospital-East, Memphis (J.D.A.).

Address reprint requests to Naftali Raz, MD, Department of Psychology, Campus Box 526400, University of Memphis, Memphis, TN 38152.

## Methods

### Subjects

The data for this study were collected in an ongoing investigation of neuroanatomic correlates of age-related differences in cognition. Subjects were recruited by advertisements placed in local media and on the University of Memphis campus. Participants signed consent forms approved by the Committee for Protection of Humans Subjects in Research of the University of Memphis and by the Baptist Memorial Hospital Patients Participation Committee and were screened by means of an extensive health questionnaire. Persons who reported a history of cardiovascular, neurologic, or psychiatric conditions; head trauma with loss of consciousness for more than 5 minutes; thyroid problems or diabetes; treatment for drug or alcohol problems, or a habit of taking more than three alcoholic drinks per day were excluded from the study. None of the participants used antiseizure medication, anxiolytics, or antidepressants. Subjects who suffered from claustrophobia were explicitly advised against participation in the study. Twelve subjects (five men and seven women, 48 to 77 years old) who reported a history of mild hypertension were admitted, because their blood pressure was successfully controlled by medication. As suggested in the literature, people who adhere to a medication regimen and control their hypertension are no more likely to exhibit signs of cerebrovascular disease than are normotensive elderly persons (15). In addition, the sample was screened for cerebrovascular disease by inspection of white matter hyperintensities on magnetic resonance (MR) imaging studies (see below for details). Of 166 subjects who underwent MR imaging, all or substantial portions of the data for eight subjects were lost owing to technical problems, such as disk failure, excessive movement artifacts, operator error, and (in two cases) significant discomfort on the part of the subjects during scanning.

All subjects were screened for dementia and depression using a modified Blessed Information-Memory-Concentration Test (16) with a cutoff score of 30 and a Geriatric Depression Questionnaire (17) with a cutoff score of 15. Finally, the MR images of all subjects admitted to the study were examined by an experienced neuroradiologist (J.D.A.) for signs of space-occupying lesions and cerebrovascular disease. After this examination, 10 subjects (six men and four women, all older than 65 years of age) were removed from the sample because of signs of mild to moderate cerebrovascular disease (numerous punctate lesions, lacunar infarcts, significant unilateral concentration of white-matter hyperintensities). Although the examination was not quantified, a conscious effort was made to render a conservative estimate of the subjects' cerebrovascular status. The final sample consisted of 146 subjects: 82 women ( $46 \pm 17$  years old) and 64 men ( $48 \pm 18$  years old). The age distribution was approximately rectangular, and did not differ between the sexes ( $t < 1$ ). Average education among the subjects was 15.8 years (more than 3 years of college), suggesting a highly selected group, and there was no correlation between education and age ( $r = .09$ , not significant [NS]). All subjects were consistent right-handers.

### MR Image Acquisition and Processing

Imaging was performed on a 1.5-T system. For each subject, the following series of images was acquired. First, a sagittal localizer sequence (three contiguous sagittal images on each side of the midsagittal plane, seven sections altogether) was obtained with parameters of 400/16/1 (repetition time/echo time/excitations) and a section thickness of 5 mm. After that, 124 contiguous axial sections were acquired using a T1-weighted three-dimensional spoiled gradient-recalled acquisition sequence. The acquisition parameters were 24/5/1, a 22-cm field of view, a  $256 \times 192$  matrix, a 1.3-mm section thickness, and a 30° flip angle. Finally, a fast spin-echo sequence of

interleaved T2- and proton density-weighted axial images was acquired for use in screening for age-related cerebrovascular disease. In this sequence, the parameters were 3300/90 effective or 18 effective/1, a 5-mm section thickness, and a 1.5-mm intersection gap.

After the images were acquired, the MR data were reformatted offline and corrected for undesirable effects of head tilt, pitch, and rotation by using proprietary software. The operator used standard neuroanatomic landmarks to bring each brain into a unified system of coordinates and to correct the deviations in all three orthogonal planes. In this standard position, the sagittal plane cut through the middle of the vermis. The axial plane, perpendicular to the sagittal, passed through the anterior-posterior commissure (incorporating the anterior-posterior commissure line) and through the orbits. The coronal plane, perpendicular to the axial, was leveled by the orbits. Reformatted images were cut into coronal and sagittal sections 1.5 mm apart and saved on a VHS tape. Thickness of the reformatted section was 0.86 mm (one linear pixel).

Morphometry was performed on a personal computer using Java software (Jandel Scientific Co, San Rafael, Calif). The MR images were digitized from the VHS tape via a Targa M-8 frame-grabber board (AT&T Corp, Murray Hill, NJ). An operator displayed each image on the 27-inch video monitor with standard brightness and contrast, and outlined the areas of interest using a digitizing tablet. The areas were computed using Java software, and the volumes of the regions of interest (ROIs) were calculated from the areas of interest and from the intersection distance.

### Delineation of the ROIs

Trained operators, who were blinded to the subjects' age and sex, manually traced all ROIs as outlined on the MR images in Figure 1. All questionable cases were resolved by consulting the correlative and general brain atlases (18, 19).

For the *cerebellar hemispheres*, the coronal sections were divided into two equal groups at random, and each half sample was traced by a different operator. The hemispheres were measured on 15 to 20 coronal sections sampled with a 3-mm gap. The vermis, the cerebellar peduncles, and the fourth ventricle were excluded, whereas the hemispheric gray matter, the cerebellar tonsils, the vellum, and the corpus medullare were included in the tracing of each cerebellar hemisphere. The rostral border was defined as the first section on which cerebellar gray matter became visible and distinguishable from the cerebellar peduncles. Distinguishing the point at which the cerebellar peduncles end and the corpus medullare begins was difficult in many cases. Therefore, an arbitrary point was used to determine when to start including the cerebellar white matter. This was the most rostral section that cut through the anterior vermis. Thus, rostral to the most rostral section of vermis, we only included the gray matter, since much of the white matter on these sections is the peduncles. In rostral-caudal progression, after the vermis was visualized, the operator included the white matter also, but excluded the vermis. The measurement proceeded until the cerebellar hemispheres were no longer observed or until they became indistinguishable from the occipital lobe of the cerebrum. Thus, the bulk of the measured volume consisted of the cerebellar gray matter from the lateral surfaces of the cerebellar hemispheres and the tonsils. The reliability of the volume measurement of the cerebellar hemispheres had an intraclass correlation, formula ICC (3), of 0.95 (20).

The *cerebellar vermis* was traced on the midsagittal section according to the rules previously described by Raz and colleagues (11). The areas of the lingua-centralis (lobules I through III), the culmen (lobules IV and V), the declive, folium, and tuber (DFT) (lobules VI and VII), and the posterior vermis (pyramis, uvula, and nodulus, or lobules VIII through X) were computed. To improve the reliability of area estimates, we combined the areas of lobules I through V and

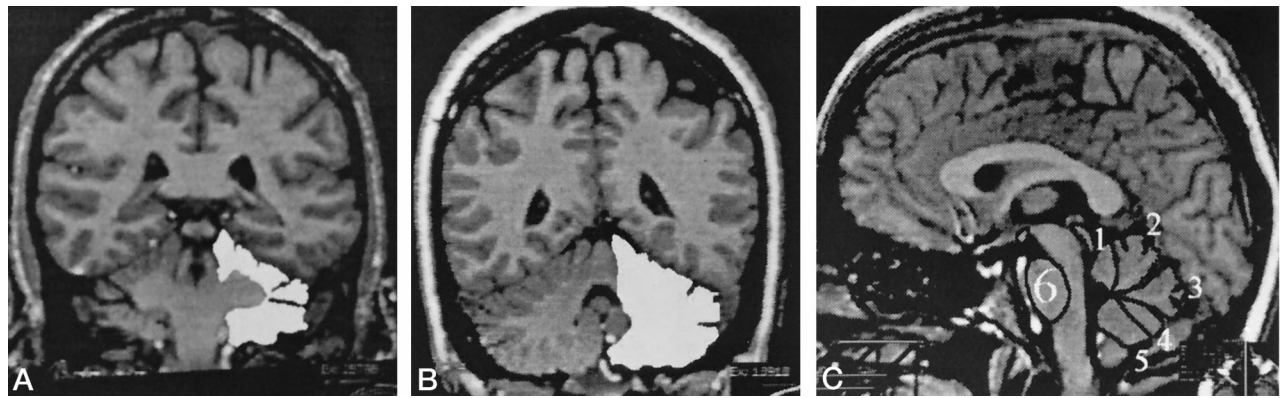


FIG 1. A, Coronal MR section at the level the splenium shows cerebellar hemispheres with the ROI traced around the cerebellar peduncles.

B, Coronal MR section shows cerebellar hemispheres. All ROIs were traced manually, and the filled-in regions are for illustration only.

C, Demarcation of the ROIs on a midsagittal section shows the vermis and the ventral pons: 1 indicates lingula-centralis; 2, culmen (anterior vermis); 3, declive, folium, and tuber; 4, pyramis; 5, uvula-nodulus (posterior vermis); 6, ventral pons.

#### Descriptive statistics and correlations for the areas and volumes of target structures and age

|                        | Age    | Height | Anterior Vermis | Declive-Folium-Tuber | Posterior Vermis | Cerebellar Hemispheres |
|------------------------|--------|--------|-----------------|----------------------|------------------|------------------------|
| Height                 | -0.01  |        |                 |                      |                  |                        |
| Anterior vermis        | -0.07  | 0.22†  |                 |                      |                  |                        |
| Declive-folium-tuber   | -0.34‡ | 0.04   | 0.38‡           |                      |                  |                        |
| Posterior vermis       | -0.23† | 0.17   | 0.37‡           | 0.35‡                |                  |                        |
| Cerebellar hemispheres | -0.32† | 0.32†  | 0.42‡           | 0.25†                | 0.37‡            |                        |
| Ventral pons           | 0.11   | 0.13   | 0.22†           | 0.06                 | 0.16             | 0.33†                  |
| Mean                   | 46.61  | 170.85 | 3.41            | 2.31                 | 3.06             | 115.05                 |
| Standard deviation     | 17.36  | 9.15   | 0.52            | 0.45                 | 0.47             | 11.80                  |

Note.—The volume of the hemispheres is in cm<sup>3</sup>, the vermian and pontine areas are in cm<sup>2</sup>, and age is in years.

†  $P < .01$

‡  $P < .001$

VIII through X into anterior and posterior vermian areas, respectively. Five segments of the vermis were measured separately. The first ROI was bound by the superior medullary vellum and the preculminate fissure, and included the lingula and lobulus centralis, lobules I through III. The second vermian ROI was the culmen (lobules IV and V), demarcated by the preculminate and primary fissures. The third ROI consisted of the DFT (lobules VI and VII), defined by the primary fissure on the superior end and the prepyramidal fissure on the posterior end. The fourth ROI was the pyramis (lobule VIII), defined by the prepyramidal and secondary fissures. The fifth ROI consisted of the uvula and the nodulus (lobules IX and X), which were located between the secondary fissure and the inferior medullary vellum. For all ROIs the upper and lower borders converged onto the apex of the fourth ventricle.

In about 10% of the cases, the uvula and the cerebellar tonsil could be clearly demarcated because of the partial voluming. In those images, we determined the borders of the fifth ROI (uvula-nodulus) by using the following approach. First, the tonsil itself was identified and the lateral borders of the tonsil were ascertained using parasagittal images adjacent to the midsagittal section. To define the lower border of the vermis, we drew an arc clockwise between the two points at which the tonsil and the vermis were discernible. Although the reliability of the five ROI measures was quite good, with intraclass correlations ranging from 0.89 to 0.94, we combined the posterior regions—pyramis, uvula, and nodulus—to raise the reliability above 0.90.

The ventral pons was easily identifiable on the midsagittal cut as an elliptical structure with an obvious ventral border. The dorsal border was the medial lemniscus, a strip of reduced

signal intensity on a T1-weighted MR image. The reliability estimates of the ventral pons area had an intraclass correlation of 0.96.

## Results

The volume of the gray matter of the cerebellar hemispheres, the total area of the vermis, the area of vermian lobules VI and VII (DFT), and the posterior vermis (but not the areas of the ventral pons and the anterior vermis) evidenced significant negative correlations with age (see Table). The mean value of the cross-sectional area of lobules VI and VII (2.31 cm<sup>2</sup>) corresponds closely to the population median value (2.60 cm<sup>2</sup>). The correspondence of the two values is especially close considering that in our approach, the area of interest was traced after the convolutions rather than by outlining the perimeter of the ROIs, as illustrated by Courchesne and colleagues (21), and was thus expected to be smaller. The volume of the cerebellar hemispheres was also close to the values reported in postmortem studies (5). The scatterplots and the age trends for all measures are depicted in Figures 2 through 6.

The magnitude of negative correlations between ROIs and age varied across vermian lobules. The strength of association between each vermian ROI

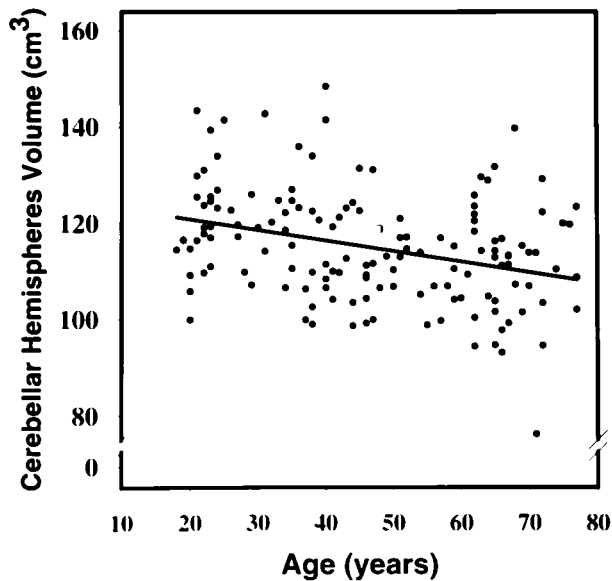


FIG 2. Regression of the volume of the cerebellar hemispheres on age. The volume is not adjusted for height and sex. Cerebellar volume =  $125.30 - 0.223 \times \text{age}$ ;  $r^2 = .10$ ;  $P < .01$ .

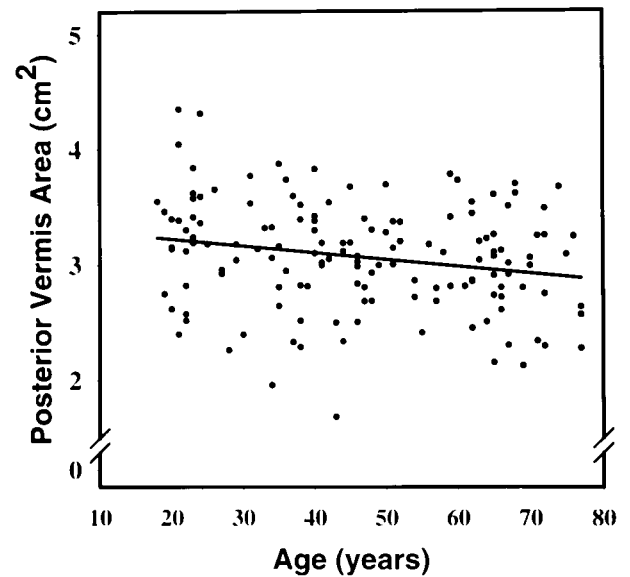


FIG 4. Regression of the area of the posterior cerebellar vermis (pyramis, uvula, and nodulus) on age. The volume is not adjusted for height and sex. Posterior vermis area =  $3.34 - 0.006 \times \text{age}$ ;  $r^2 = .05$ ;  $P < .01$ .

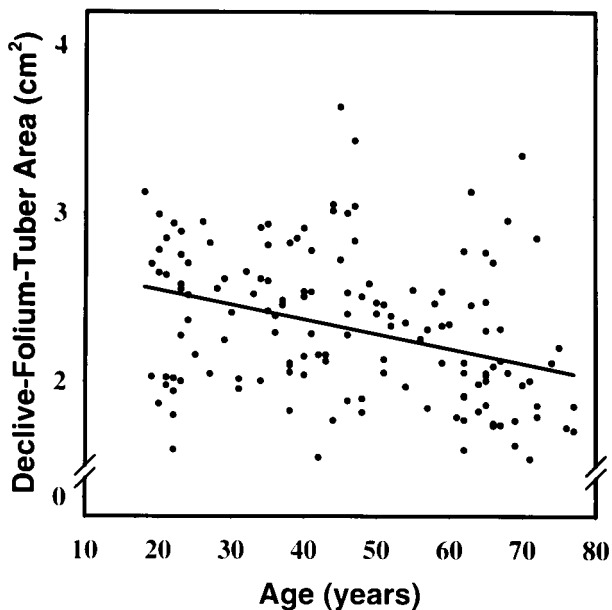


FIG 3. Regression of the volume of the declive-folium-tuber (DFT) on age. The volume is not adjusted for height and sex. DFT area =  $2.72 - 0.008 \times \text{age}$ ;  $r^2 = .12$ ;  $P < .001$ .

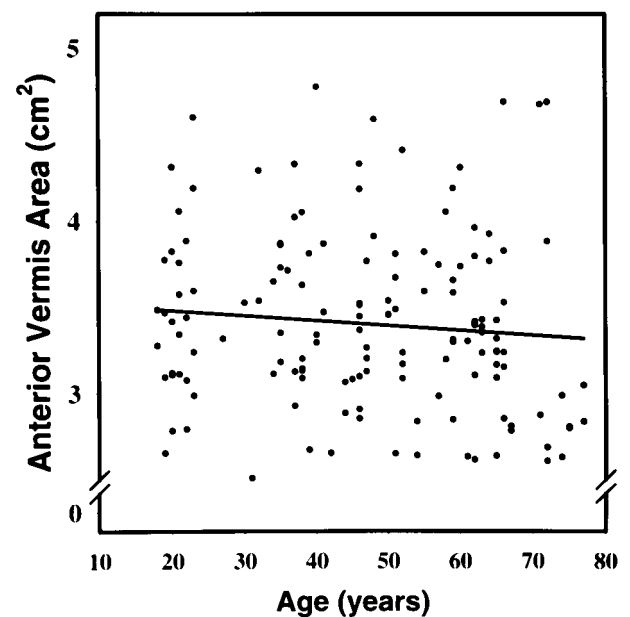


FIG 5. Regression of the area of the anterior cerebellar vermis (lingula, centralis, and culmen) on age. The volume is not adjusted for height and sex. Anterior vermis area =  $3.54 - 0.003 \times \text{age}$ ;  $r^2 = .01$ , NS.

and age were compared by using Steiger's formula (22), which takes into account the correlations among the ROIs. As predicted, the correlation between age and the area of the DFT was significantly larger than the next closest correlation (between the posterior vermis area and age):  $Z^* = 1.71$ ;  $P < .05$ , one-tailed. The difference was even greater for the correlation between age and the anterior vermis area:  $Z^* = 3.07$ ;  $P < .001$ , one-tailed.

Using a simple regression of the area on age, we estimate that within the age span of 20 to 80 years,

linear decline in the area of the most vulnerable lobules (VI and VII) amounts to 4% per decade. The cerebellar hemispheres and the posterior vermis were affected by age to a lesser degree than was the DFT area. According to the regression analysis of this sample data, the volumes of the cerebellar hemispheres and the posterior vermis are expected to shrink by only about 2% per decade; the corresponding rate for the anterior vermis is only 0.5% per decade.

To examine sex differences in the aging of posterior



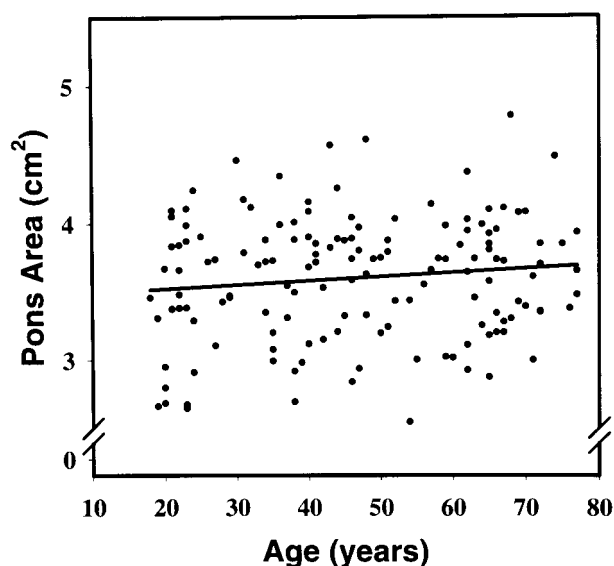


FIG 6. Regression of the area of the ventral pons on age. The volume is not adjusted for height and sex. Pons area =  $3.46 - 0.003 \times \text{age}$ ;  $r^2 = .01$ , NS.

fossa structures we analyzed the areas of the vermian lobules and the pons, and the volume of the cerebellar hemispheres in three general linear models. In each model, the volume or area of the ROI served as the dependent variable, sex was a grouping factor, age (recentered at the sample mean) was a continuous independent variable, and height (also recentered at the sample mean) served as a covariate. Because men were significantly taller than women ( $178 \pm 6$  cm versus  $165 \pm 7$  cm,  $t(144) = 11.89$ ;  $P < .001$ ), we introduced height into all models as a covariate to control for variations that could have been related to the differences in body size. Cerebellar hemispheres (right versus left) and three vermian ROIs were repeated measures in their respective models. The assumption of homogeneity of regression slopes was met for all models (height  $\times$  sex interaction  $F < 1$ ).

The results of these analyses revealed significant main effects of age on the volume of both cerebellar hemispheres:  $F(1,142) = 21.42$ ;  $P < .001$ . The age-related shrinkage of the vermis was also significant:  $F(1,142) = 12.12$ ;  $P < .001$ . A significant age  $\times$  lobule interaction ( $F[2,284] = 3.13$ ;  $P < .05$  with Greenhouse-Geisser correction) confirmed the differences in age trends observed for unadjusted measures of the vermian regions.

Although there were no sex differences in the total vermian area, significant lobule  $\times$  sex interaction ( $F[2,284] = 7.04$ ,  $P < .001$  with Greenhouse-Geisser correction) indicated that men had differentially larger vermian lobules even after adjustment for height. The post-hoc  $t$  tests revealed no sex differences in the areas of the posterior vermis and lobules VI and VII ( $t[144] = 1.61$ , and  $t[144] = 1.05$ , respectively, both NS), whereas the anterior vermian area was larger in men:  $t(144) = 3.07$ ;  $P < .005$ . The volume of the cerebellar hemispheres was also greater in men:  $F(1,142) = 9.05$ ;  $P < .005$ , although

the effect of sex was not equivalent across the hemispheres ( $F[1,142] = 6.55$ ;  $P < .05$  for the hemisphere  $\times$  sex interaction). The observed hemispheric volume differential between the sexes was small but reliable. The left hemisphere was larger in men by 6.5%, whereas the right hemisphere was larger by 7.9%. For the ventral pons area, neither age ( $F[1,142] = 1.59$ ) nor sex ( $F < 1$ ) had a significant effect.

## Discussion

An awareness of normal neuroanatomic variability is important for understanding pathologic changes. In regard to the posterior fossa structures, the cumulative research record of in vivo studies is rather short and there is a need for normative data. In our prospective study, we examined two potential sources of normal variability in regional cerebellar volumes: age and sex. The results of this investigation provide a valuable addition to the normative database of the cerebellar anatomy in that they support the notion of differential aging of the cerebellum and the ventral pons: mild but significant age-related shrinkage of the neocerebellar vermis (lobules VI and VII) and the cerebellar hemispheres contrasts with the apparent age invariance of the anterior vermis and the ventral pons.

Some of our previous findings were not replicated. For example, we observed no age-related shrinkage of the culmen yet noted a mild decline in the area of lobules VIII through X, a departure from our previous observation in a mostly archival sample (11). Such discrepancies underscore the need for accumulation of a reasonably large sample of studies, in which each study's outcome is represented by its effect size and is treated as a single observation. Only a metaanalysis (23) of multiple studies can yield meaningful estimates of the magnitude of age and sex differences in cerebellar anatomy. In the metaanalytic context, "failures to replicate" are simply instances of effects that are not significantly different from zero. Sufficient accumulation of zero effects and a zero mean effect indicate that nonzero findings are only incidental and do not reflect the central tendency.

It is noteworthy that these age-related differences were observed in a sample of highly educated and healthy subjects. Such a sample is hardly representative of the general population, and clinical generalizability of our findings is limited. The goal of this investigation was to test the hypothesis regarding differential aging of the cerebellum under the most favorable circumstances. The results show that even so-called successful aging (24) is associated with mild shrinkage of the selected cerebellar regions.

It is unclear what mechanisms account for the observed patterns of differential vulnerability to aging. An examination of the histologic findings of the aging cerebellum shows general but not differential atrophy, as the age-related loss of Purkinje cells is uniformly distributed across the vermian lobules and the cerebellar hemispheres (4). Whatever the causes of selective vulnerability of the cerebellar lobules VI and

VII, they are not necessarily specific to aging, for a similar differential pattern has been observed in infantile autism (25), Down syndrome (26), and acute childhood leukemia (27).

One possible cause of differential aging may be age-related changes in the cerebrovascular system, although at present, the relevant evidence is mixed. Normal aging, especially when accompanied by mild hypertension, is associated with significant cerebrovascular disease. Reduction in cardiac output (28, 29), vascular responsiveness (30), cerebral blood flow (31), and flow velocity (32), as well as progressive deterioration of cerebral vessels (33) and disorganization of the cerebellar arterial networks (34), are observed throughout life. On the other hand, in contrast to associated cerebral cortices, the cerebellum, when examined in toto, shows no significant age-related declines in blood flow, oxygen consumption, and glucose metabolism (35–38).

The topography of its blood supply may predispose the cerebellum to differential aging. The vulnerable regions, the lateral surface of the cerebellar hemispheres and the posterior vermis, are supplied by the tributaries of the posterior inferior cerebellar artery (PICA), which originates in the vertebral artery, whereas the blood supply for the age-invariant superior vermis comes from the superior cerebellar artery, which branches off the basilar artery (39, 40). As the vertebral system receives a relatively small volume of blood even under normal circumstances (41), and age-related vertebral insufficiency is rather common (42), the cerebellar structures that are the most remote from the source may be at the greatest risk. Indeed, the PICA territory is the most common location for cerebellar infarcts (43), although the distribution of infarcts by the distance from the PICA origin is unknown. It is possible that under conditions of insufficient perfusion, the border-zone (watershed) areas may suffer the most from transient subclinical ischemia and hypoxia. This possibility, although purely speculative, merits further investigation with special attention to evaluation of regional cerebrovascular variations within the cerebellum.

Our finding of larger cerebellar hemispheres in men is in accord with the bulk of the literature (44), and it mirrors analogous observations in the cerebral cortex (3). In contrast, a similar trend in the anterior vermis has not been reported, and must be viewed with greater caution, as it may be a spurious finding. Even for well-replicated sex differences in brain morphology, the causes and mechanisms remain to be elucidated. These differences are most likely of prenatal or perinatal origin, because in contrast to sex differences in body size, sexual dimorphism of cerebral and cerebellar size is observed in children before puberty (45) and cannot be attributed to postpubertal differences in sex hormones. Future exploration of sex differences in brain morphogenesis in utero may shed light on gross neuroanatomic differences that are observed apparently throughout the normal life span.

## Conclusions

We found that normal aging selectively affects the cerebellar hemispheres as well as lobules VI and VII and VIII through X of the cerebellar vermis while sparing the anterior vermis and the ventral pons. These observations are noteworthy as they demonstrate that the central nervous system is not spared even in successful aging. Although the degree of apparent loss of cerebellar tissue is rather mild and unlikely to be noticed on clinical examination, it should be taken into account in functional imaging studies of aging, when the cerebellum is considered as a suitable structure for reference and normalization (35–38). These findings also raise a question of the relationship between age-related decline in multiple sensorimotor and cognitive functions believed to be subserved by the cerebellum (25, 42) and deterioration of their neuroanatomic substrates.

## Acknowledgment

We gratefully acknowledge the cooperation of the medical and technical staff of the Baptist MR Diagnostic Imaging Center, Memphis, Tenn.

## References

1. Kemper TL. **Neuroanatomical and neuropathological changes during aging and in dementia.** In: Albert ML, Knoepfel EJE, eds. *Clinical Neurology of Aging*. 2nd ed. New York, NY: Oxford University Press; 1994:3–67.
2. Raz N. **Neuroanatomy of aging brain: evidence from structural MRI.** In: Bigler ED, ed. *Neuroimaging II: Clinical Applications*. New York, NY: Academic Press; 1996: 153–182.
3. Raz N, Gunning FM, McQuain JM, et al. **Selective aging of human cerebral cortex observed in vivo: differential vulnerability of the prefrontal gray matter.** *Cereb Cortex* 1997;7:268–282.
4. Ellis RS. **Norms for some structural changes in human cerebellum from birth to old age.** *J Comp Neurol* 1920;32:1–33.
5. Torvik A, Torp S, Lindboe CF. **Atrophy of the cerebellar vermis in ageing: a morphometric and histological study.** *J Neurol Sci* 1986; 76:283–294.
6. Escalona PR, McDonald WM, Doraiswamy M, et al. **In vivo stereological assessment of human cerebellar volume: effects of gender and age.** *AJNR Am J Neuroradiol* 1991;12:927–929.
7. Schaefer GB, Thompson JN, Bodensteiner JB, Gingold M, Wilson M, Wilson D. **Age-related changes in the relative growth of the posterior fossa.** *J Child Neurol* 1991;6:15–19.
8. Luft AR, Skalej M, Klockgether T, Voigt K. **Aging and gender do not affect cerebellar volume in humans.** *AJNR Am J Neuroradiol* 1997;18:593–594.
9. Weis S, Kimbacher M, Wenger E, Neuhold A. **Morphometric analysis of the corpus callosum using MRI: correlation of measurements with aging in healthy individuals.** *AJNR Am J Neuroradiol* 1993;14:637–645.
10. Nishimiya J. **CT evaluation of cerebellar atrophy with aging in healthy persons.** *No To Shinkei* 1988;40:585–591.
11. Raz N, Torres IJ, Spencer WD, White K, Acker JD. **Age-related regional differences in cerebellar vermis observed in vivo.** *Arch Neurol* 1992;49:412–416.
12. Shah SA, Doraiswami PM, Husain MM, et al. **Assessment of posterior fossa structures with midsagittal MRI: the effects of age.** *Neurobiol Aging* 1991;12:371–374.
13. Shah SA, Doraiswami PM, Husain MM, et al. **Posterior fossa abnormalities in major depression: a controlled magnetic resonance imaging study.** *Acta Psychiatr Scand* 1992;85:474–479.
14. Hayakawa K, Konishi Y, Matsuda T, et al. **Development and aging of the brain midline structures: assessment with MRI imaging.** *Radiology* 1989;172:171–177.
15. Fukuda H, Kitani M. **Difference between treated and untreated hypertensive subjects in the extent of periventricular hyperintensities observed on brain MRI.** *Stroke* 1995;26:1593–1597.

16. Blessed G, Tomlinson BE, Roth M. **The association between quantitative measures of dementia and senile change in the cerebral grey matter of elderly subjects.** *Br J Psychiatry* 1968;114:797-811
17. Radloff LS. **The CES-D scale: a self-report depression scale for research in the general population.** *Appl Psychol Measur* 1977;1:385-401
18. Courchesne E, Press GA, Murakami J, et al. **The cerebellum in sagittal plane: anatomic-MRI correlation 1: Vermis.** *AJNR Am J Neuroradiol* 1989;10:659-665
19. Nieuwenhuys R, Voogd J, Huijzen C. **The Human Central Nervous System: A Synopsis and Atlas.** 3rd ed. Berlin, Germany: Springer; 1988
20. Shrout PE, Fleiss JL. **Intraclass correlations: uses in assessing raters reliability.** *Psychol Bull* 1979;86:420-428
21. Courchesne E, Yeung-Courchesne R, Egaas B. **Methodology in neuroanatomical measurement.** *Neurology* 1994;44:203-208
22. Steiger JH. **Tests for comparing elements of a correlation matrix.** *Psychol Bull* 1980;87:245-251
23. Hedges L, Olkin I. **Statistical Methods for Meta-Analysis.** Orlando, Fla: Academic Press; 1985
24. Rowe JW, Kahn RL. **Human aging: usual and successful.** *Science* 1987;237:143-149
25. Courchesne E. **A neurophysiological view of autism.** In: Schopler E, Mesibov G, eds. *Neurobiological Issues in Autism.* New York, NY: Plenum; 1987:285-384
26. Raz N, Torres IJ, Briggs SD, et al. **Selective neuroanatomical abnormalities in Down's syndrome and their cognitive correlates: evidence from MRI morphometry.** *Neurology* 1995;45:356-366
27. Cieselski KT, Yanofsky R, Ludwig RN, et al. **Hypoplasia of the cerebellar vermis and cognitive deficits in survivors of childhood leukemia.** *Arch Neurol* 1994;51:985-993
28. Shock NW. **Some physiological aspects of aging in man.** *Bull N Y Acad Med* 1956;2:268-283
29. Shimada K, Miyashita H, Nishinaga M, Kuroda T. **The hemodynamics of elderly hypertension.** *Nippon Ronen Igakkai Zasshi* 1994;31:916-920
30. Sato N, Kiuchi K, Shen YT, Vatner SF, Vatner DE. **Adrenergic responsiveness is reduced, while baseline cardiac function is preserved in old adult conscious monkeys.** *Am J Physiol* 1995;269:H1664-H1671
31. Meyer JS, Shaw TG. **Cerebral blood flow in aging.** In: Albert ML, ed. *Clinical Neurology of Aging.* New York, NY: Oxford University Press; 1984:178-196
32. Arnolds BJ, von Reutern GM. **Transcranial Doppler sonography: examination technique and normal reference values.** *Ultrasound Med Biol* 1986;12:115-123
33. Weber G, Bianciardi G, Bussani R, et al. **Atherosclerosis and aging: a morphometric study on arterial lesions of elderly and very elderly necropsy subjects.** *Arch Pathol Lab Med* 1988;112:1066-1070
34. Akima M, Nonaka H, Kagesawa M, Tanaka K. **A study on the microvasculature of the cerebellar cortex: the fundamental architecture and its senile change in the cerebellar hemisphere.** *Acta Neuropathol (Berl)* 1987;75:69-76
35. Kushner M, Tobin M, Alavi A, et al. **Cerebellar glucose consumption in normal and pathologic states using fluorine-FDG and PET.** *J Nucl Med* 1987;28:1667-1670
36. Marchal G, Rioux P, Petit-Taboué MC, et al. **Regional cerebral oxygen consumption, blood flow, and blood volume in healthy human aging.** *Arch Neurol* 1992;49:1013-1020
37. Loessner A, Alavi A, Lewandrowski KU, Mozley D, Souder E, Gur RE. **Regional cerebral function determined by FDG-PET in healthy volunteers: normal patterns and changes with age.** *J Nucl Med* 1995;36:1141-1149
38. Moeller JR, Ishikawa T, Dhawan V, et al. **The metabolic topography of normal aging.** *J Cereb Blood Flow Metab* 1996;16:385-398
39. Lister JR, Rhoton AL Jr, Matsushima T, Peace DA. **Microsurgical anatomy of the posterior inferior cerebellar artery.** *Neurosurgery* 1982;10:170-199
40. Hardy DG, Peace DA, Rhoton AL Jr. **Microsurgical anatomy of the superior cerebellar artery.** *Neurosurgery* 1980;6:10-28
41. Boyajian RA, Schwend RB, Wolfe MM, Bickerton RE, Otis SM. **Measurement of anterior and posterior circulation flow contributions to cerebral blood flow: an ultrasound-derived volumetric flow analysis.** *J Neuroimaging* 1995;5:1-3
42. Baloh RW. **Neurotology of aging: vestibular system.** In: Albert ML, ed. *Clinical Neurology of Aging.* New York, NY: Oxford University Press; 1984:345-361
43. Marinkovic S, Kovacevic M, Gibo H, Milisavljevic M, Bumbasirevic L. **The anatomical basis for the cerebellar infarcts.** *Surg Neurol* 1995;44:450-460
44. Raz N. **A comment on Luft et al.** *AJNR Am J Neuroradiol* 1997;18:594-595
45. Giedd JN, Snell JW, Lange N, et al. **Quantitative magnetic resonance imaging of human brain development: ages 4-18.** *Cereb Cortex* 1996;6:551-560